

UV-assisted desalination of seawater using titanium dioxide nanotube doped polyether block amide membrane

F. U. Nigiz and M. E. Kibar

ABSTRACT

In this study, a UV-assisted desalination system was prepared with a non-porous TiO₂-doped Pebax 1657 membrane. The membranes were characterized and desalination tests were performed. The effects of UV light and TiO₂ ratio on the performance of desalination were investigated. According to the results, TiO₂ incorporation increased the membrane hydrophilicity, increased the membrane swelling values, enhanced the membrane flux and improved the salt rejection. Moreover, UV treatment has a positive effect on desalination performance. The best improvement was achieved in the results of 10 wt.% TiO₂-doped membrane. It was found that the flux value of the UV-treated membrane having 10 wt.% TiO₂ concentration was 8.2 kg/m²-h and the salt rejection value was 99.97%. It was found that the prepared membrane showed excellent desalination performance.

Key words | desalination, non-porous membrane, Pebax 1657 membrane, TiO₂ nanopowder

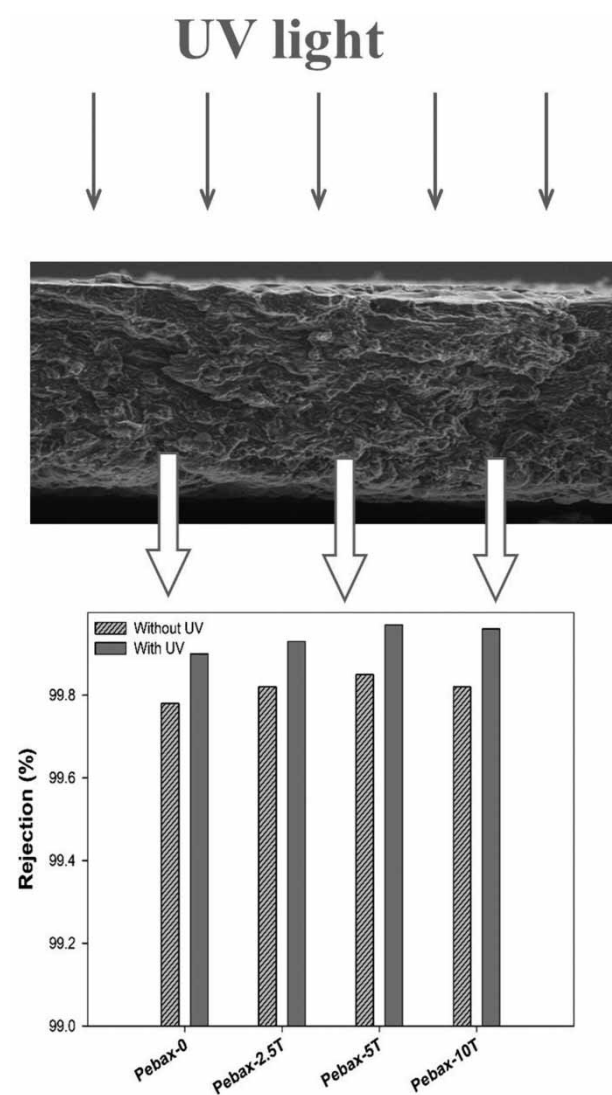
F. U. Nigiz (corresponding author)
Chemical Engineering Department of Çanakkale
Onsekiz Mart University,
Çanakkale,
Turkey
E-mail: filiz.ugur@gmail.com;
filiz.ugur@comu.edu.tr

M. E. Kibar
Chemical Engineering Department of Kocaeli
University,
Kocaeli,
Turkey

HIGHLIGHTS

- Photocatalytic membrane reactor (PMR) was tested for desalination with/without UV.
- In this study TiO₂-doped Pebax 1657 membrane was used in PMR.
- TiO₂ nanotube incorporation enhanced the flux from 4.11 kg/m²-h to 8.2 kg/m²-h.
- The conductivity of the pure water was improved from 206 µs to 21 µs by UV irradiation.

GRAPHICAL ABSTRACT



INTRODUCTION

Photocatalytic oxidation of organic compounds for desalination and water treatment is one of the most interesting topics of recent years. The activity of this reaction depends on the process and the photocatalyst type. There are two main process configurations, as a process with free catalyst and as a process where the catalyst is immobilized on a support. The activity of the catalyst used in the free state is high, but after the water treatment, it is necessary to remove the

catalyst to eliminate the poisoning effect of the catalyst. The use of photocatalytic membrane reactors (PMR) restricts the reduction of photocatalytic activity and ensures that the freshwater is not poisoned by the photocatalyst (Zheng *et al.* 2017; Argurio *et al.* 2018). Membrane usage prevents the passage of the catalyst into the purified water side. Additionally, the use of photocatalytic membrane reactors eliminates the use of further separation steps such as

sedimentation–coagulation–flocculation, which will then be used to separate the photocatalyst. Furthermore, it reduces the total process volume and enables the reuse of the catalyst. The heat energy which is necessary for the reaction and separation can be provided by the UV in daylight. Therefore, the PMR system is defined as an energy-saving and cost-effective purification process (Mozia 2010; Molinari *et al.* 2017).

The photocatalytic membrane has been recently developed for a wide range of application (Zheng *et al.* 2017; Argurio *et al.* 2018; Ye *et al.* 2019). Biological treatment of organic content water, seawater desalination, and wastewater treatments are the best-known application areas of photocatalytic membranes. The mechanical properties and selective separation capability of membranes can be destroyed by the accumulation of organic pollutants in seawater. Therefore, photocatalytically eliminating organic pollutants may improve both the structural properties and separation performance of membranes (Yacou *et al.* 2015).

Membrane technology is an emerging science for advanced water treatment. Membranes are mostly used for water purification, wastewater treatment, and desalination purposes. The productivity and overall performances of membrane-based processes are directly related to the physico-chemical properties of the membranes. Therefore, scientific studies have been focused on the development of high-performance membrane materials. Especially for water treatment, it is important to produce superior membranes having high water permeability, high rejection capacity, bio-fouling resistance, and process stability. For this purpose, new-generation composite membranes have been developed.

In this study, the aim is to develop a new material for UV-assisted desalination of seawater. For this purpose, titanium dioxide nanotube (TiO₂)-doped polyether block amide (PEBA-Pebax 1657 (commercial name)) membrane has been produced. According to the authors' knowledge, TiO₂-Pebax nanocomposite membrane is prepared here for the first time for the purpose of photocatalytic desalination. Different from the literature, the membrane is used as a non-porous form to remove water. Hence, the separation mechanism is based on water–membrane affinity. Therefore, any improvement by addition of TiO₂ is much more important. TiO₂ is the most widely used photocatalyst. TiO₂ is a semiconducting material that destroys organic contaminants in water with the assistance of UV-light (Yacou *et al.* 2015;

Solcova *et al.* 2016; Al Mayyahi 2018). However, because the energy band of TiO₂ is large, it is not active in daylight. Since the UV content in daylight does not exceed 5%, a UV source is required for photocatalytic activation. In this study, the desalination system has been utilized by assisting UV light. The structural property of the composite membrane has been investigated by means of Fourier transform infrared spectroscopy and X-ray diffraction. The distribution of TiO₂ particles within the membrane has been analysed using polarized electron microscopy (POM) and scanning electron microscopy (SEM). Swelling experiments have been performed to determine the water-uptake capacity of the TiO₂ filled and unfilled Pebax 1657 membrane. The separation performance of membranes with/without TiO₂ nanotubes was investigated to separate water seawater. Desalination tests have been conducted at room temperature with/without UV light. The effect of TiO₂ concentration and UV light were investigated.

EXPERIMENT

Titanium dioxide nanotube preparation

One gram of commercial titanium dioxide powder (Acros, Thermo Fisher Scientific, USA) was mixed with 10 M sodium hydroxide solution. The mixture was subjected to an ultrasonic bath for 30 minutes. The mixture was left for hydrothermal treatment at 130 °C for 24 hours in a Teflon-lined autoclave. After filtration, the nanotube titanium dioxide was washed with hydrochloric acid and water. Nanotube titanium dioxide was dried at 110 °C for 16 hours and calcined at 500 °C for 2 hours.

Membrane preparation

Polyether block amide (Pebax 1657) was kindly supplied from Arkema, France, and 10 wt.% of Pebax-acetic acid solution was prepared and stirred until the solution became homogeneous. The determined amount of TiO₂ nanotube particles was added to the Pebax solution according to the weight of the dry Pebax polymer. According to the Pebax content, TiO₂ concentration in the membrane solvent was changed from 0 to 10 wt.%. Membranes were denoted

according to the TiO₂ content in the membrane. Pebax-0 represents the membrane without filler, Pebax-2.5T represents the membrane having 2.5 wt.% of TiO₂ nanotube particles. Membrane solutions were cast onto a Teflon plate and allowed to dry at room temperature. Then, membranes were cured in a vacuum oven at 60 °C. The membrane was then immersed in a solution containing 2 vol.% of tolylene-2,4-diisocyanate-hexane solution to prevent the dissolving of the membrane in the water media.

Swelling experiment

Swelling experiments were performed to determine the affinity of the membranes to the water. The swelling test was continued for approximately four hours until the membrane reached a constant weight. For the swelling experiment, the membranes were cut into equal size (1 cm²) and were soaked in deionized water. The dry (M_d) and swollen (M_s) weights of the membranes were measured and the swelling percentages (S) were determined by the following equation:

$$S(\%) = \frac{M_s - M_d}{M_d} * 100 \quad (1)$$

Desalination

Desalination tests were carried out under ambient conditions. Prior to desalinating the seawater, the separation capabilities of membranes were tested to separate water from seawater. Water removal and water flux were calculated from Equations (2) and (3), which are shown as follow (Nigiz & Hilmioğlu 2016):

$$R(\%) = \frac{C_i - C_f}{C_i} * 100 \quad (2)$$

$$F = \frac{M}{t.A} \quad (3)$$

where M (kg) is the weight of permeate water on the downstream side of the membrane, t is the operating time (h), A is the effective membrane area (m²), and C_i and C_f represent the initial and final total dissolved solid concentrations of water. Total dissolved solids and ion concentrations were analysed using multi-functional conductometry (Seven Compact,

Mettler Toledo). The seawater desalination test was conducted under UV light and the effect of UV on desalination was investigated.

Characterization

The crystalline phases were characterized by means of X-ray diffraction (XRD) (Rigakku, Miniflex 2, Japan). The 2θ values were selected from 10° to 80° with a step size of 0.02 using Cu K α radiation ($\lambda = 0.15418$ nm) at 45 kV/40 mA. Fourier transform infrared spectroscopy was used to determine the chemical structure of the membrane in the wavelength range from 650 cm⁻¹ to 4,000 cm⁻¹ (Perkin Elmer ATR). Surface hydrophilicity properties of the membranes were determined using contact angle measurements (Attension).

RESULTS

Characterization results of membranes

The prepared membranes were characterized in order to determine physical, chemical and morphological properties. In Figure 1, the XRD spectra of the prepared pure nanotube TiO₂ and nanotube TiO₂-doped membrane are given. The characteristic peaks of the anatase phase are obtained at 2 θ 25.1°, 36.9°, 37.7°, 38.4°, 47.9°, 53.7° and 54.9° degrees. The characteristic peaks are determined at 12.3° and 21.4° for Pebax.

In the literature, Pebax is defined as a semi-crystalline polymer which shows diffraction peaks at 2θ 14°, 17° and 26° (Sridhar *et al.* 2008). As seen from the figure, there are no crystalline phases obtained from nanotube-doped Pebax. This is due to the chemical interaction of Pebax with nanotube TiO₂. Nanotubes affected the chemical bonds and an amorphous phase was formed.

The FTIR analysis of TiO₂-nanoparticle-doped Pebax 1657 membrane is given in Figure 2. The bands at 1,107 and 1,733 cm⁻¹ are attributed to the C–O–C and –C=O stretching vibrations, respectively. Also, another two bands at 1,638 and 3,303 cm⁻¹ are assigned to the presence of H–N–C=O and N–H groups, in the hard polyamide (PA) segment, respectively. In the FTIR spectrum of Pebax, it seems that the PA block of Pebax is significantly self-associated via hydrogen bonding.

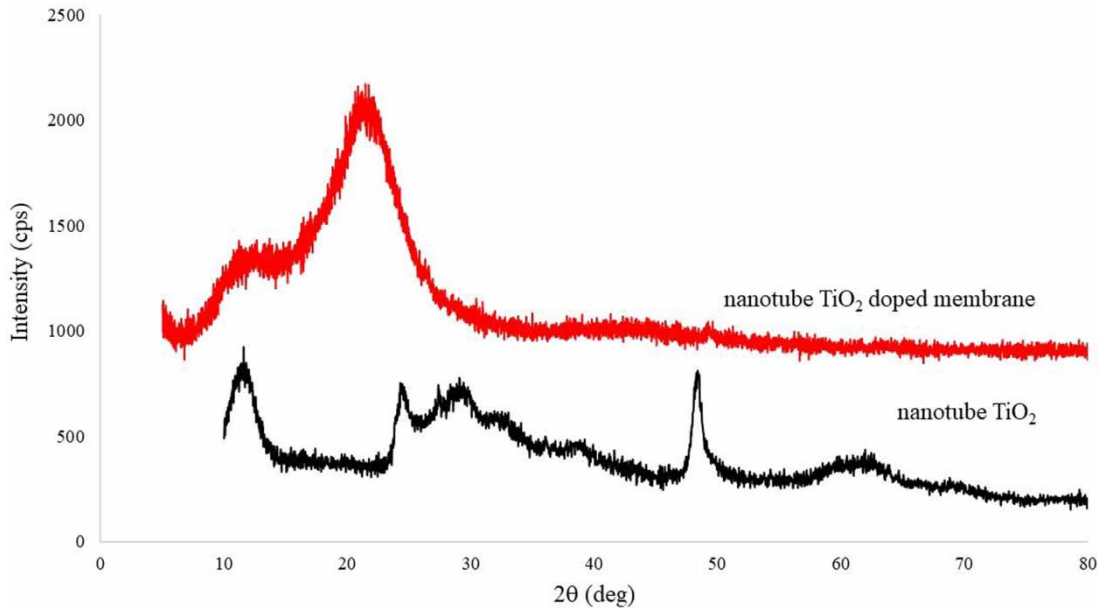


Figure 1 | XRD patterns of Pebax-nanotube TiO_2 membrane and pure nanotube TiO_2 .

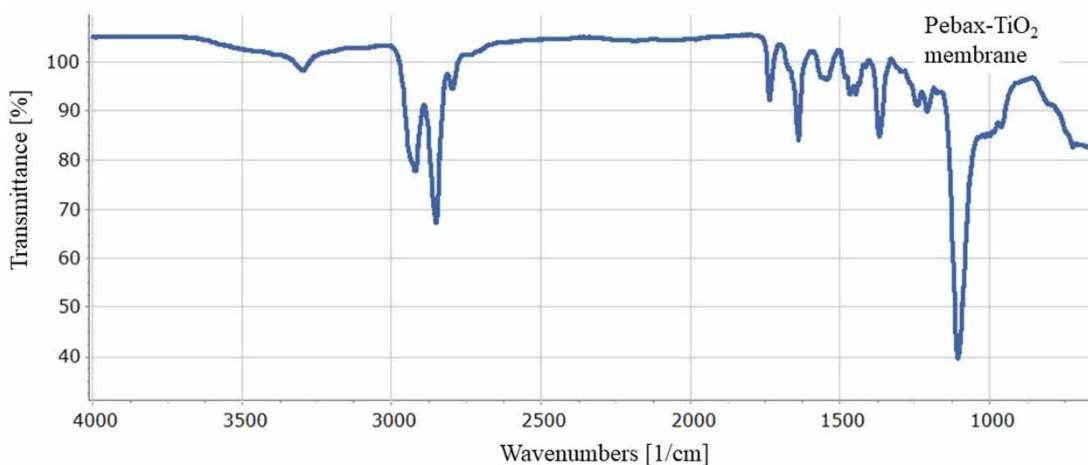


Figure 2 | FTIR spectra of Pebax- TiO_2 membrane.

Figure 3 shows FTIR spectra of commercial and nanotube TiO_2 particles. The bands which are observed in the range of $3,500$ to $3,200\text{ cm}^{-1}$ are related to the asymmetric and symmetric stretching vibrations of hydroxyl ($-\text{OH}$) groups. The $\text{Ti}-\text{OH}$ stretching mode is observed at $1,633.58\text{ cm}^{-1}$ (Chougala *et al.* 2017) which is in agreement with the literature.

Figure 4 shows the distribution of TiO_2 particles in the membrane. The first picture represents the Pebax 1657 membrane without filler, and the smooth, dense structure of the membrane can be clearly observed except for some

impurity in the surface. The membrane has a non-porous structure. The POM images of the 2.5 wt.% TiO_2 -loaded membrane indicated that the distribution of the particles within the membrane is excellent. Homogeneous distribution of the additive into the membranes is very important in terms of providing the same physical and chemical properties in every region on the membrane. Homogeneous dispersion means uniform separation performance across the membrane. As is known, there are electrostatic interactions between particles, such as TiO_2 ,

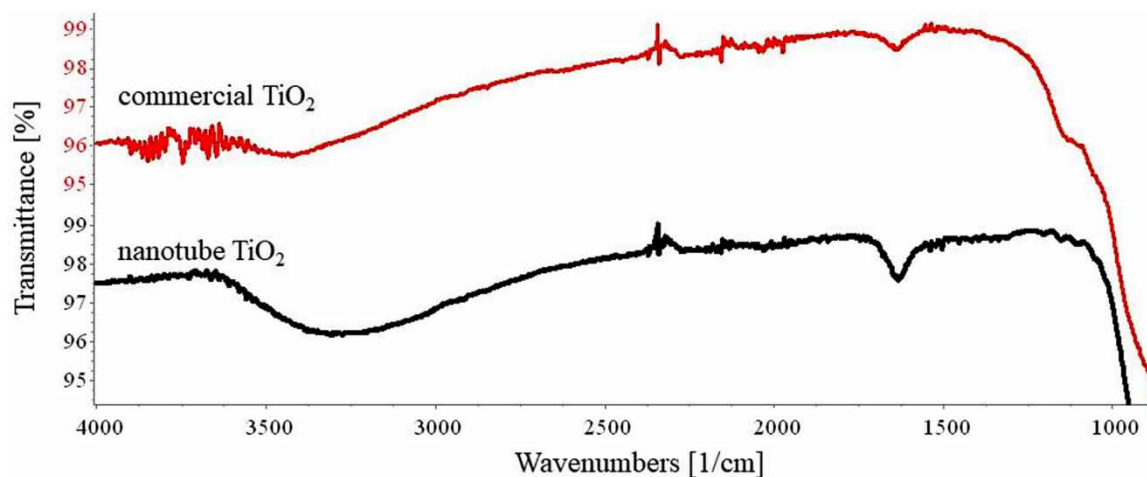


Figure 3 | FTIR spectra of commercial and nanotube TiO_2 .

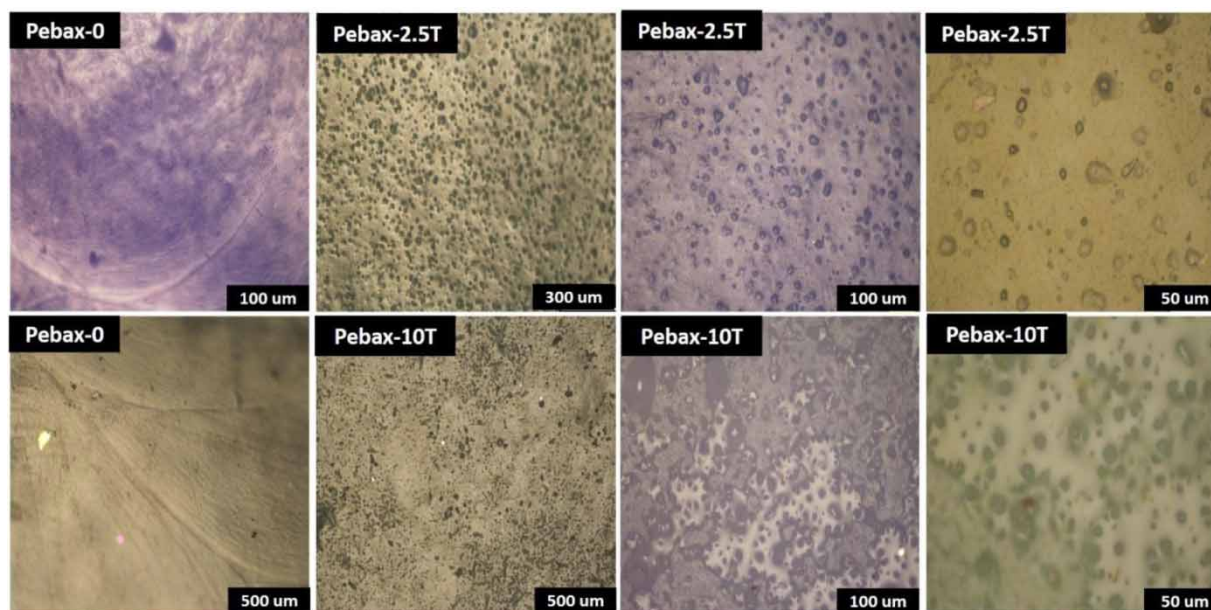


Figure 4 | Polarized electron microscopy images of the pristine and TiO_2 -loaded membranes.

which tend to connect with each other. In this study, the particles were separated from each other by the sonication process, and then the priming method was used to provide the homogeneous distribution (Nigiz 2018). Thus, agglomeration was prevented. Agglomeration within the membrane was rarely observed even when the concentration of TiO_2 (wt.10%) was high. However, it is still possible to see accumulated TiO_2 particles in a particular area. This is due to the orientation of the particles in the drying step of the membrane. During the casting–evaporation step, the membranes

were first dried under room conditions. The TiO_2 particles might be orientated at this stage.

In Figure 5, the cross-sectional views of the membranes are clearly seen. SEM images of 10 wt% TiO_2 -loaded membranes are given with different magnification. The uniform distribution of TiO_2 is seen in Figure 5. The nanotube diameters vary from 10 to 23 nm and the nanotubes contribute to the properties of the membrane.

The contact angle between the membrane surface and water droplet is shown in Table 1. It is clear that the water

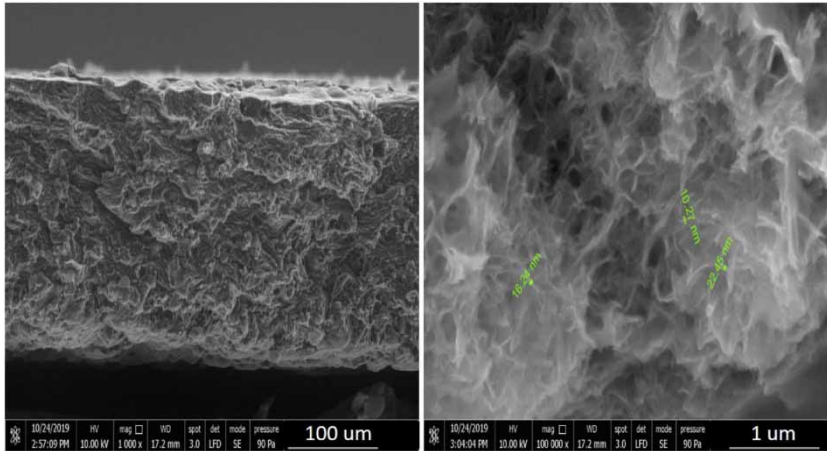


Figure 5 | SEM images of TiO₂-loaded membranes.

Table 1 | Contact angle of membranes with water droplets

| | Membrane code | | | |
|-------------------|---------------|------------|----------|-----------|
| | Pebax-0 | Pebax-2.5T | Pebax-5T | Pebax-10T |
| Contact angle (°) | 68 | 57 | 49 | 38 |

contact angle decreases with increasing TiO₂ ratio in the membrane. This means that the hydrophilicity of the membrane is enhanced with TiO₂ addition. Owing to the hydrophilicity of

TiO₂ particles, the surface water affinity of the membrane is enhanced as also reported by Huang *et al.* (2017). According to the results obtained from the contact angle experiments, water flux is expected to increase as TiO₂ ratio increases in the membrane matrix. There have also been many studies on the use of TiO₂ in the membrane matrix to enhance the surface hydrophilicity and flux, as well (Du *et al.* 2017; Pan *et al.* 2019).

Figure 6 shows the water affinity of the pristine and TiO₂-nanotube-loaded membranes in terms of the swelling

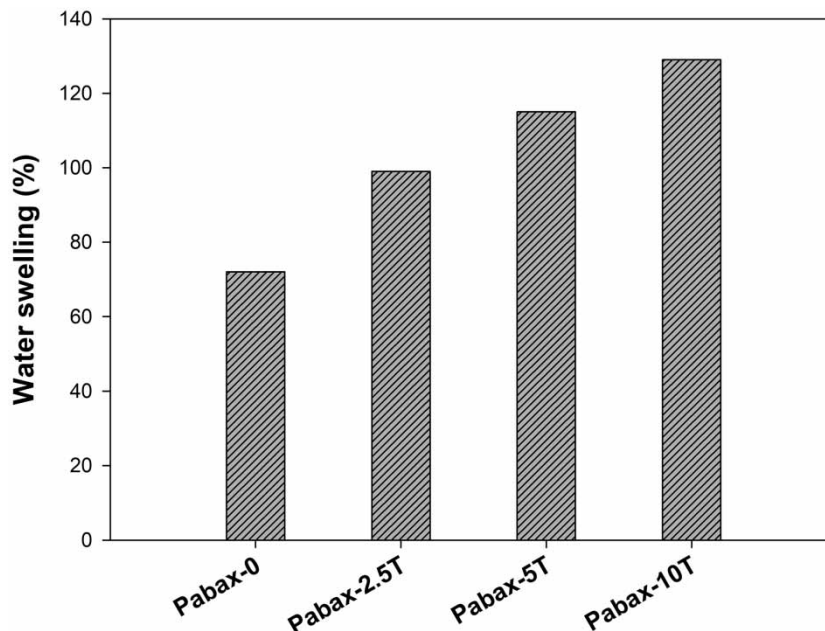


Figure 6 | Swelling results of the membranes.

experiment. The increasing TiO₂ nanotube ratio remarkably enhanced the water swelling ratio. The swelling values of the membrane increased from 72% to 129% when the TiO₂ ratio was increased from 0 wt.% to 10 wt.%. This is due to the hydrophilic character of TiO₂ nanotube particles, which was also confirmed by the results of the water contact angle experiments. It has been reported that TiO₂ nanotube particles, and especially nano-sized TiO₂ nanotubes, have an affinity to water (Bolis *et al.* 2012).

Desalination results in the system with/without UV lamps are given in Figure 7 as a function of flux and rejection. In order to investigate the effect of TiO₂ nanotube addition, a desalination experiment on the pristine Pebax 1657 (Pebax-0) was also performed. As can be seen from the figure, increasing TiO₂ ratio improved flux values significantly. In the pristine membrane, a 4.11 kg/m²·h flux value was obtained while 8.2 kg/m²·h flux was obtained with 10 wt.% TiO₂-nanotube-loaded membrane when the separation occurred in the UV-assisted system. As was confirmed by the results of surface hydrophilicity and swelling degree, the water permeability was increased due to the hydrophilic character of the TiO₂ nanotube particles. At the same time, it was also found that UV usage has little effect on the flux results. In the pristine membrane, 3.75 kg/m²·h flux was obtained in the system without using UV light and this value increased to 4.11 kg/m²·h when UV light was used. The increase in flux is related to the UV effect on organic compounds in seawater. By using UV light, TiO₂ was activated and the degradation of organics contributed to preventing surface cake formation. Therefore,

flux decrement due to the boundary layer problem could be prevented. This effect could become more effective in long-period separation experiments. Another reason could be related to the antimicrobial effect of TiO₂ on bacteria, microbial and other substances in seawater. These substances also cause cake formation on the membrane surface. TiO₂ is known as an anti-microbial chemical that prevents biological contamination on membrane surfaces.

The effect of TiO₂ ratio on the salt rejection of the desalination process performed with/without UV light is seen in Figure 8. All Pebax-based membranes show a high salt rejection value above 99.78%. TiO₂ incorporation into the membrane appears to increase salt rejection. The possible reason for these minor differences is that the TiO₂ particles extend the tortuous pathway, increase the water affinity of the membrane, and increase the ion rejection by electrostatic interaction. The higher salt rejection values are seen in the system where the UV lamp is used. This should be attributed to the retention of ions by TiO₂, which generates radicals by UV activation. The highest salt rejection value was obtained as 99.97% with 10 wt.% TiO₂-loaded membrane. The conductivity of the permeated water was decreased from 206 µs to 21 µs by applying the UV light.

CONCLUSIONS

In this study, TiO₂-nanotube-incorporated Pebax 1657 non-porous membranes were produced. The produced

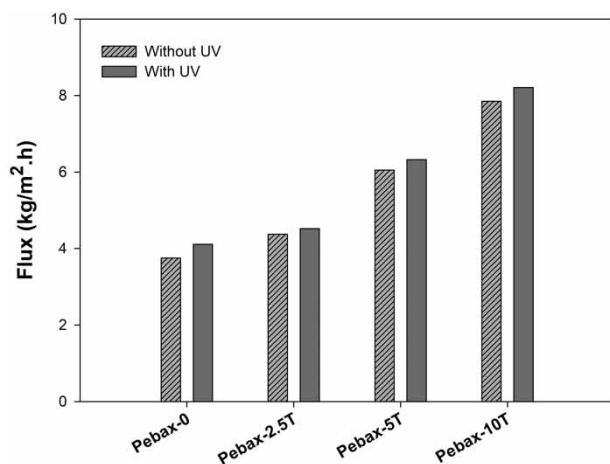


Figure 7 | Flux results of the membranes.

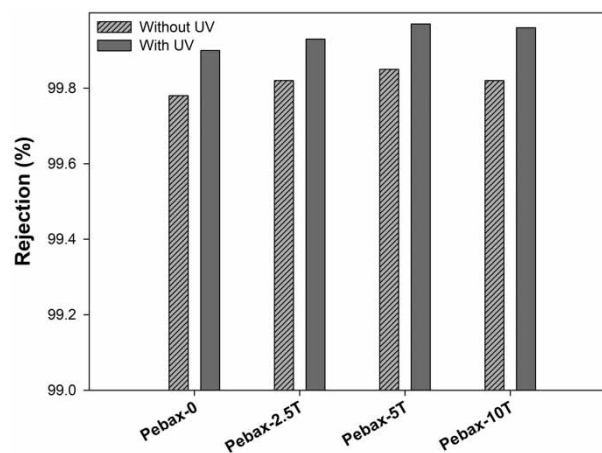


Figure 8 | Rejection results of the membranes.

membranes were characterized and the desalination performance of the pristine and nanocomposite membranes was carried out at room temperature. General experimental results can be summarized as follows:

- The compatibility of Pebax 1657 polymer and TiO₂ nanotube particles was excellent and the TiO₂ nanotube particles were homogeneously dispersed in the matrix.
- TiO₂ nanotube incorporation was found to increase both the surface and structural hydrophilicity of the membrane. The swelling values of the membrane increased from 72% to 129% when the TiO₂ ratio was increased from 0 wt.% to 10 wt.%.
- TiO₂ nanotube addition enhanced the flux from 4.11 kg/m²·h to 8.2 kg/m²·h and the salt rejection from 99.90% to 99.97%.
- Both the flux and salt rejection values were improved with assistance of UV light.

ACKNOWLEDGEMENTS

The authors would like to thank colleagues from the Polymer and Rubber Technology: Characterization Laboratory, Kocaeli University, for their support on use of characterization equipment. This work was supported by Kocaeli University Scientific Research Projects Coordination Unit, Project Number FBA-2019/1552.

REFERENCES

- Al Mayyahi, A. 2018 TiO₂ polyamide thin film nanocomposite reverses osmosis membrane for water desalination. *Membranes* **8**, 66.
- Argurio, P., Fontananova, E., Molinari, R. & Drioli, E. 2018 Photocatalytic membranes in photocatalytic membrane reactors. *Processes* **6**, 162.
- Bolis, V., Busco, C., Ciarletta, M., Distasi, C., Erriquez, J., Fenoglio, I., Livraghi, S. & Morel, S. 2012 Hydrophilic/hydrophobic features of TiO₂ nanoparticles as a function of crystal phase, surface area and coating, in relation to their potential toxicity in peripheral nervous system. *Journal of Colloid and Interface Science* **369**, 28–39.
- Chougala, L. S., Yatnatti, M. S., Linganagoudar, R. K., Kamble, R. R. & Kadadevarmath, J. S. 2017 A simple approach on synthesis of TiO₂ nanoparticles and its application in dye sensitized solar cells. *Journal of Nano- and Electronic Physics* **9**, 04005.
- Du, Y., Li, Y. & Wu, T. 2017 A superhydrophilic and underwater superoleophobic chitosan–TiO₂ composite membrane for fast oil-in-water emulsion separation. *RSC Adv.* **7**, 41838–41846.
- Huang, L., Jing, S., Zhuo, O., Meng, X. & Wang, X. 2017 Surface hydrophilicity and antifungal properties of TiO₂ films coated on a Co-Cr substrate. *BioMed Research International* **2017**, 2054723.
- Molinari, R., Lavorato, C. & Argurio, P. 2017 Recent progress of photocatalytic membrane reactors in water treatment and in synthesis of organic compounds. A review. *Catalysis Today* **281**, 144–164.
- Mozia, S. 2010 Photocatalytic membrane reactors (PMRs) in water and wastewater treatment. A review. *Separation and Purification Technology* **73**, 71–91.
- Nigiz, F. U. 2018 Preparation of high-performance graphene nanoplate incorporated polyether block amide membrane and application for seawater desalination. *Desalination* **433**, 164–171.
- Nigiz, F. U. & Hilmioglu, N. D. 2016 Pervaporative desalination of seawater by using composite and blended poly(vinyl alcohol) membranes. *Desalination and Water Treatment* **57**, 4749–4755.
- Pan, Z., Cao, S., Li, J., Du, Z. & Cheng, F. 2019 Anti-fouling TiO₂ nanowires membrane for oil/water separation: synergetic effects of wettability and pore size. *Journal of Membrane Science* **572**, 596–606.
- Solcova, O., Spacilova, L., Maletterova, Y., Morozova, M., Ezechias, M. & Kresinova, Z. 2016 Photocatalytic water treatment on TiO₂ thin layers. *Desalination and Water Treatment* **57** (25), 11631–11638.
- Sridhar, S., Smitha, B., Suryamurali, R. & Aminabhavi, T. M. 2008 Synthesis, characterization and gas permeability of an activated carbon-loaded PEBAX 2533 membrane. *Designed Monomers & Polymers* **11** (1), 17–27.
- Yacou, C., Smart, S. & Diniz da Costa, J. C. 2015 Mesoporous TiO₂ based membranes for water desalination and brine processing. *Separation and Purification Technology* **147**, 166–171.
- Ye, G., Yu, Z., Li, Y., Li, L., Song, L., Gu, L. & Cao, X. 2019 Efficient treatment of brine wastewater through a flow-through technology integrating desalination and photocatalysis. *Water Research* **157**, 134–144.
- Zheng, X., Shen, Z. P., Shi, L., Cheng, R. & Yuan, D. H. 2017 Photocatalytic membrane reactors (PMRs) in water treatment: configurations and influencing factors. *Catalysts* **7** (8), 224.

First received 14 November 2019; accepted in revised form 22 May 2020. Available online 5 June 2020